2-4 Supercontinuum Generation and its Applications

SOTOBAYASHI Hideyuki

In this paper, a design theory for the supercontinuum spectrum generation in an optical fiber is firstly described. To generate a wideband supercontinuum spectrum, the balance between fiber nonlinearity and the amount of group velocity dispersion is important. Secondly, the experimental results of supercontinuum generation are shown. A few kinds of optical fibers such as a highly nonlinear dispersion-shifted fiber and a highly nonlinear bismuth-oxide fiber are tested. Finally several applications of supercontinuum light are described. We demonstrate multi-wavelength light source, multiplexing format conversion, and optical characterization using a supercontinuum light source.

Keywords
Photonic processing, Nonlinear optics, Ultrafast phenomena, Photonic network, Photonic sensing

1 Introduction

Ultrafast photonic processing is expected to play a major role in the photonic networks and photonic sensing systems. At the bandwidth of 100 GHz or above, electronics imposes severe technology and economic constraints, which ultrafast photonic processing could advantageously remove. The quasi-instantaneous response of Kerr nonlinearity in fibers makes it the most attractive effect to overcome bandwidth limitations. For simplicity, consider two optical beams of different wavelength co-propagating in the same optical fiber, the intensity dependence of the refractive index leads to a large number of interesting nonlinear effects; self-phase modulation (SPM), cross-phase modulation (XPM), and four-wave mixing (FWM). These ultrafast phenomena could be favorably applied to photonic processing. One application is optical multiplexing, which is used as optical switches, multiplexers, and demultiplexers. Another possible application is wavelength conversion, which is to be used in a variety of WDM systems. Supercontinuum (SC) generation is the other promising technique for a various applications in photonic networks and sensing systems.

In this paper, the design theory of the supercontinuum generation in an optical fiber is described and the experimental demonstrations are shown. Some applications of supercontinuum light source are discussed.

2 Supercontinuum generation

2.1 Design theory of supercontinuum generation

The techniques to generate supercontinuum in optical fibers are roughly divided into two categories. One is spectrum broadening by the pulse compression using soliton effects in an anomalous dispersion fiber. Another is the spectrum broadening by the accumulation of frequency chirping caused by optical Kerr effects in a normal dispersion fiber. There are important advantages of the latter technique

over the former one. Nonlinear pulse propagation in an anomalous dispersion fiber tends to generate multiple pulses with complex frequency chirping variation. The spectral variation and noise associated with some supercontinuum spectra cause difficulty in some applications. Anomalous dispersion fiber generally generates the broader spectra, but it is often structured and noisy due to pulse breakup, modulation instability and other nonlinear effects. On the other hand, smooth, unstructured spectra can be produced with a normal dispersion fiber. The output pulse after propagation in a normal dispersion fiber is a single pulse keeping its high coherency. Frequency chirping is almost linear up-chirping.

Supercontinuum generation process in a normal dispersion fiber is described by the nonlinear Shrödinger equation, including the second order dispersion and Kerr effect. The ratio of $\sqrt{L_d / L_{nl}}$, where L_d is the dispersive length, and L_{nl}, the nonlinear length, governs the amount of spectral broadening achievable in a normal dispersion fiber [1]-[3]. The spectral broadening factor roughly proportional to $\sqrt{L_d / L_{nl}}$. The dispersive length can be written as $L_d = \tau_0^2/\beta_{av}$, where τ_0 is the pulse width parameter and β_{av}, the average dispersion. The nonlinear length is defined as, $L_{nl}=1/\gamma P_0$, where P_0 is the peak power of the input excitation, and γ the nonlinear index coefficient. The nonlinear index coefficient, γ, is defined as $\gamma = 2\pi n_2/\lambda A_{eff}$, where n_2 is the nonlinear refractive index coefficient, λ, the wavelength, and A_{eff}, the effective area of the fiber. Thus, $\sqrt{L_d / L_{nl}}$ can be written as $\sqrt{(2\pi n_2 \tau_0^2 P_0/\lambda A_{eff} \beta_{av})}$. Therefore, the spectral broadening can be improved by increasing the nonlinear index coefficient of the fiber, or through using pulses with high peak powers. The nonlinear index coefficient can be increased by the use of a material with high nonlinearity or a reduction in fiber effective area. Dispersion limits the maximum amount of spectral broadening possible, but the supercontinuum generated is still smooth and controlled.

2.2 Supercontinuum generation in a normal dispersion fiber

We tested a highly nonlinear fiber with normal dispersion for supercontinuum generation[3]. The bismuth-oxide fiber we used has a core diameter of 1.7 μm and an effective area of 3.3 μm^2. The nonlinear coefficient is approximately 1100 +/− 15% $(W\text{-}km)^{-1}$, about 400 times larger than that of standard dispersion-shifted single mode fiber[4]. The high nonlinearity is due to the highly nonlinear nature of the bismuth-oxide glass material, approximately an order of magnitude larger than standard silica fiber, and the small effective area The normal dispersion value was −250 ps/nm/km. The refractive index of the core is 2.22, and that of the cladding 2.13 at 1550 nm. As shown in Fig. 1, an optical parametric oscillator (OPO), producing 150-fs pulses centered at the wavelength of 1540 nm is used as the signal source. It is synchronously pumped by a Ti:Sapphire laser, at a repetition rate of 82 MHz. The output of the OPO is coupled into a 3-cm length of single-mode fiber, which serves as a spatial filter. Next, the light from the SMF is re-collimated and focused into a 2-cm long highly nonlinear bis-

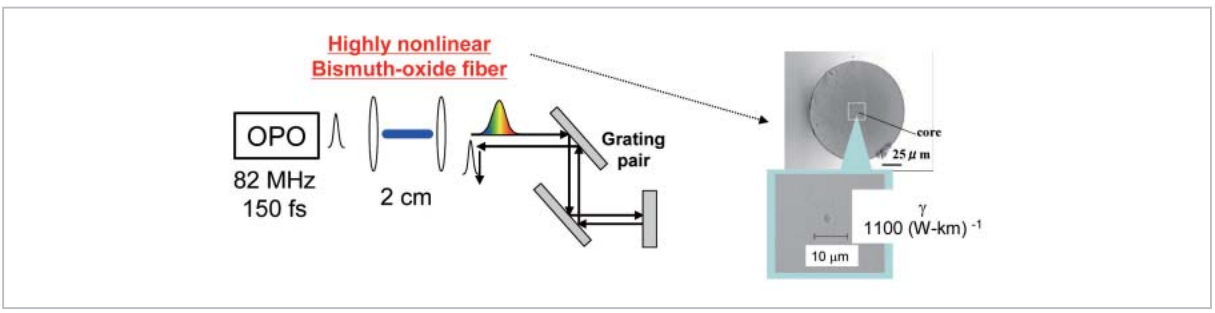

Fig. 1 *Experimental setup*

muth-oxide fiber. The coupling loss was 6 dB. Figure 2 shows the spectra produced from a 2-cm piece of fiber as a function of the input power. By increasing the input power, the spectrum broadened wider. For a 32 mW of input average power, spectrum is generated from 1300 nm to >1700 nm, with a 3-dB spectral width of 170 nm. The pulse width was broadened to 865 fs. Figure 3 shows the autocorrelation trace of the compressed pulse using a grating pair, providing -6400 fs^2 of dispersion. Two gold 75-lines/mm gratings, separated by 8.5 cm, were used to compress the pulses. The pulses were compressed to 25 fs. The time-bandwidth product of our compressed pulses, assuming a sech pulse envelope, was 0.49. Higher order chirp as well as the roll-off in spectral efficiency of the gratings for wavelengths shorter than 1500 nm probably limits the compressed pulsewidth.

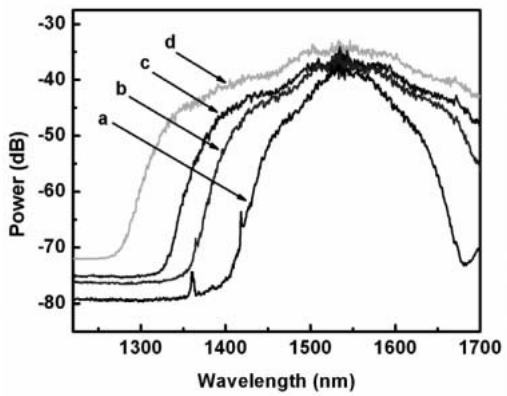

Fig.2 *Spectra from a 2-cm long fiber generated by 1540-nm excitation at average powers exiting the fiber of: a) 32 mW b) 21.4 mW c) 14 mW d) 7 mW*

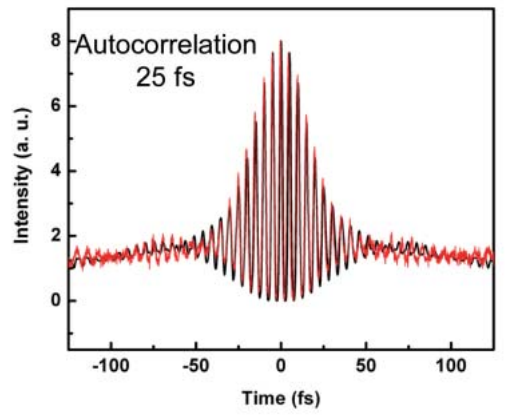

Fig.3 *Autocorrelation trace of compressed pulse*

2.3 Supercontinuum generation in an anomalous dispersion fiber

An anomalous dispersion fiber was tested for supercontinuum generation[4]. Figure 4 shows the experimental setup. A femtosecond stretched-pulse fiber-laser is used as a seed pulse source, which uses a 55.6 cm bismuth-oxide erbium-doped fiber (Bi-EDF) as a gain medium. The Bi-EDF was bi-directionally pumped with two 975 nm di odes. The power of each pump laser was set to 350 mW. Because the dispersion of the Bi-EDF was high in normal dispersion, a 1.8 m of low nonlinear single-mode fiber (LNL-SMF) was used to control the cavity dispersion. The dispersion value of the LNL-SMF was 20.64 ps/nm/km at 1550 nm and the effective core area was 113.3 μm^2. The dispersion variation around the cavity led to stretch-pulse mode-locking through nonlinear polarization rotation[4]. The center wavelength of the laser output was 1571 nm and the spectral width was 58 nm. The repetition rate and the output power of the laser were 34.2 MHz and 28.8 mW, respectively. In order to compress the pulse, the laser output was coupled into 1.8 m of LNL-SMF. The pulse width of the laser output was 1.57 ps and it was compressed to 100 fs. A 500 m long highly nonlinear dispersion-shifted fiber (HNL-DSF) had a zero-dispersion wavelength

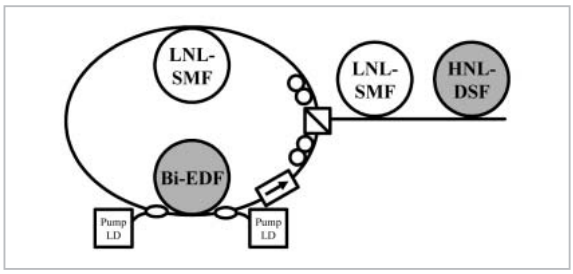

Fig.4 *Experimental setup*

(LNL-SMF: low nonlinear single-mode fiber, Bi-EDF: Bismuth-oxide based Erbium-doped fiber, LD: Laser diode, HNL-DSF: High-nonlinear dispersion shifted fiber)

of 1565 nm and the nonlinear coefficients of 21 km^{-1} W^{-1}. Figure 5 shows the generated supercontinuum spectrum. In the longer wavelength region above 1750 nm, the spectrum was characterized using a spectrometer. Although the spectrum had many dips, with pulse energies of 840 pJ, a broadband spectrum spanning from 1.2 to 2.0 μm was generated in an anomalous dispersion fiber.

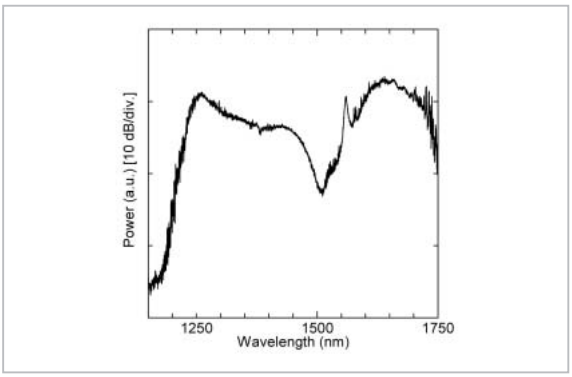

Fig.5 *Generated supercontinuum spectrum.*

3 Multi-wavelength signal generation

A simultaneous multi-wavelength signal generation is demonstrated by use of a supercontinuum spectrum. The scheme uses a single supercontinuum source, which is directly pumped by an optically multiplexed currier suppressed return-to-zero (CS-RZ) signal[5]. Figure 6 shows the experimental setup. A 40 Gbit/s CS-RZ was multiplexed by using an optical multiplexer integrated as a planar lightwave circuit (PLC). A 10 Gbit/s, 1.5 ps RZ signal is optically time-delayed multiplexed into a 40 Gbit/s signal. The optical carrier phase of each delayed adjacent pulse is shifted by π using optical phase shifters. Simultaneous multi-wavelength 40 Gbit/s CS-RZ multiplications are performed by supercontinuum generation directly pumped by a 40 Gbit/s CS-RZ signal at 1530.3 nm. Supercontinuum is generated in a 2 km long supercontinuum fiber (SCF)[6].By spectrum slicing of supercontinuum using an arrayed waveguide grating (AWG) with a 100 GHz channel spacing, simultaneous multi-wavelength SC-RZ can be generated (ch. 1: 1535.04 nm - ch. 81: 1600.60 nm). A tellurite-based EDFA (T-EDFAs) were used for amplification of the continuous signal band in the C- and L-bands. The transmission lines were two pairs of a single mode dispersion fiber and a reversed dispersion fiber (RDF). The total length was 80 km. Signals were wavelength demultiplexed by 100 GHz spacing, 81 channels of AWG. Figure 7 shows the optical spectra of supercontinuum at the output of SCF (upper trace), signals before transmission (middle trace), and after transmission and amplified by

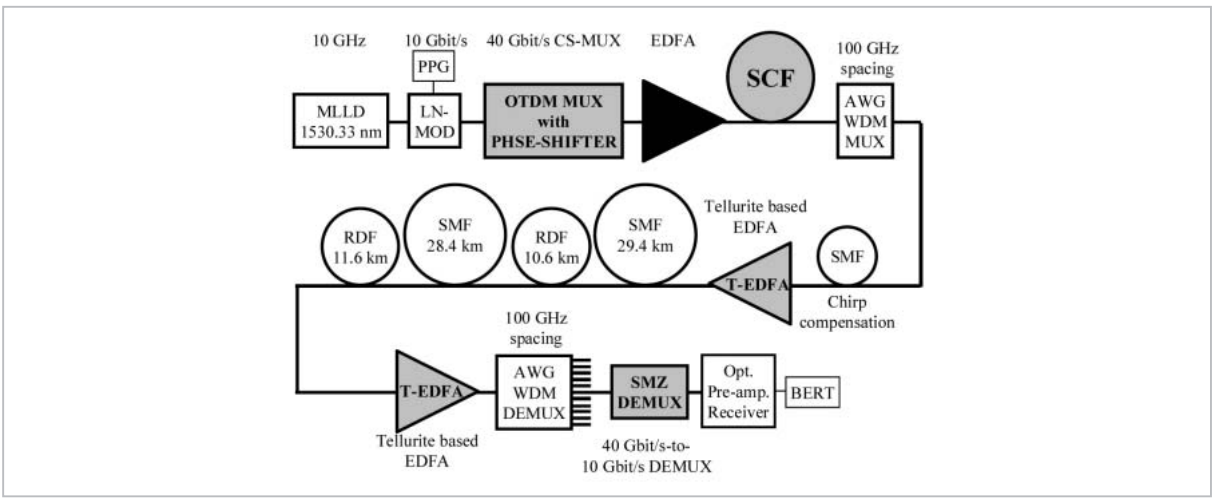

Fig.6 *Experimental setup. (LNL-SMF: low nonlinear single-mode fiber, Bi-EDF: Bismuth-oxide based Erbium-doped fiber, LD: Laser diode, HNL-DSF: High-nonlinear dispersion shifted fiber)*

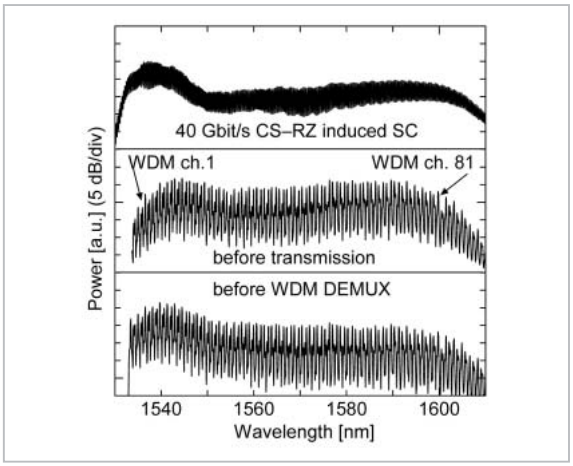

Fig.7 *(a) Measured optical spectra of SC at the output of the SCF (upper trace), signals before transmission (middle trace), and signals after transmission and amplified by a T-EDFA (lower trace).*

the T-EDFA (lower trace). The power difference in all WDM channels after 80 km transmission and amplified by a T-EDFA was about 7 dB. For all measured channels, the BERs were less than 1×10^{-9}.

4 Multiplexing format conversion

Multiplexing format conversion and reconversion of OTDM and WDM are demonstrated by use of a supercontinuum generation[7]. A 40 Gbit/s OTDM-to-4 × 10 Gbit/s WDM-to-40 Gbit/s OTDM conversions are experimentally demonstrated. The operation principle of the multiplexing conversion of TDM-to-WDM-to-TDM is illustrated in Fig. 8. The conversion scheme is based upon ultrafast photonic processing both in the time domain and frequency domain, that is, optical time-gating along with time-shifting in the time domain, and supercontinuum generation followed by spectrum-slicing in the frequency domain. A 40 Gbit/s OTDM signal in the time slot T_i (i=1,2,3,4) itself generates a supercontinuum, yielding a multi-wavelength 40 Gbit/s TDM signal in the same time slot as shown in Fig. 8(b). The generated supercontinuum is spectrum-sliced at WDM channel wavelengths of λ_i (i=1,2,3,4) as shown in Fig. 8(c). Each WDM signal is time-shifted so that the time position of T_i at λ_i aligns within the same time-flame as shown in Fig. 8(c). Finally, they are optically time-gated at 10 GHz repetition rate. Thus, each 40 Gbit/s TDM data in the time slot T_i is converted into 4 × 10 Gbit/s WDM data of λ_i in order as shown in Fig. 8(d)[7][8]. As for WDM-to-TDM conversion, each of four WDM signals is time-shifted to position a WDM signal of λ_i is located at a time-flame of T_i as shown in Fig. 8(f). Multiplexed 4 × 10 Gbit/s WDM signals serve to generate another supercontinuum as shown in Fig. 8(g). By spectrum-slicing the supercontinuum at the original wavelength of λ_0, 4 × 10 Gbit/s WDM signals are simultaneously reconverted into a 40 Gbit/s TDM signals as shown in Fig. 8(h). Figure 9 shows the experimental setup of

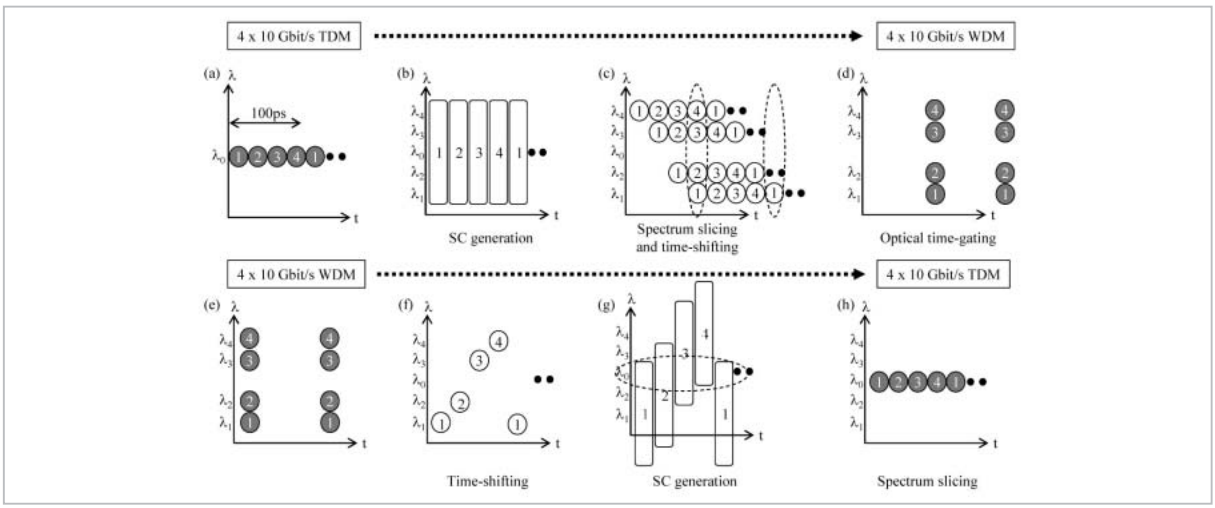

Fig.8 *Operational principle of conversion and reconversion of OTDM-to-WDM-to-OTDM*

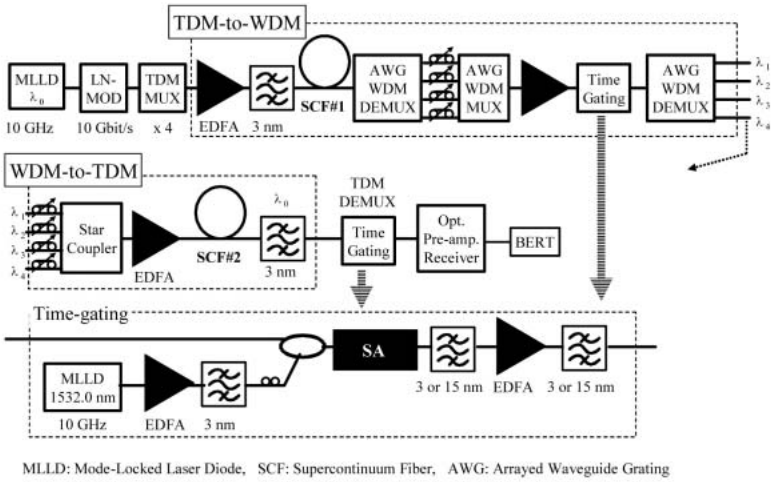

Fig.9 *Experimental setup*

40 Gbit/s TDM-to-WDM-to-TDM conversions[7]. In the OTDM-to-WDM conversion, 40 Gbit/s data at λ_0(=1553.9 nm) was generated by four time multiplexing of 10 Gbit/s signals. A supercontinuum spectrum is generated in SCF#1[6]. An AWG having channel spacing of 350 GHz is used for 4 WDM (λ_1: 1549.7 nm–λ_4: 1558.2 nm) multiplexing/demultiplexing.

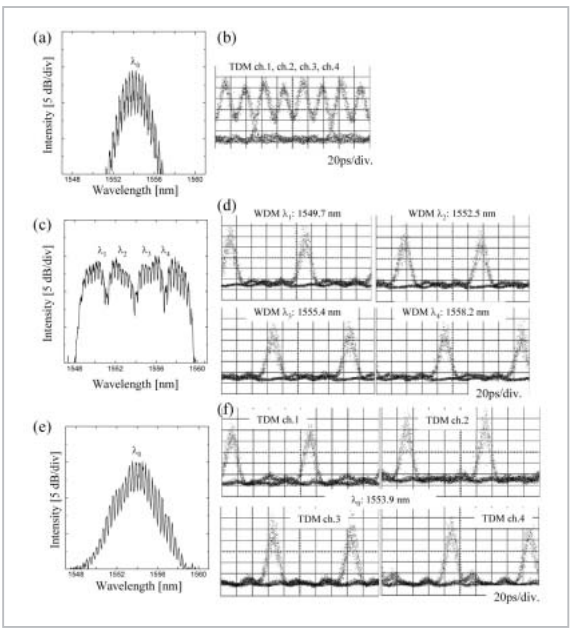

Fig.10 *(a) optical spectrum and (b) eye diagram of original 40 Gbit/s TDM, (c) optical spectra and (d) eye diagram of converted 4x 10 Gbit/s WDM, and (e) optical spectrum and (f) eye diagram of reconverted 40 Gbit/s TDM*

The time positions of WDM channels at λ_1–λ_4 are individually aligned using optical delay lines as shown in Fig. 8(c). The time-gating at the repetition rate of 10 GHz was carried out by using a semiconductor SA, which was driven by a 10 GHz repetition rate, 2 ps width pulse train at 1532 nm. Optical time-gated signal was WDM demultiplexed using the 4-ch., 350 GHz spacing AWG. Thus, 4×10 Gbit/s OTDM-to-WDM was accomplished. Regarding with WDM-to-TDM reconversion, after the time positions of WDM channels at λ_1–λ_4 are individually aligned such that shown in Fig. 8(f) using optical delay lines, 4×10 Gbit/s WDM signals were multiplexed using a star coupler. Supercontinuum spectrum is generated in SCF#2. The generated multi-wavelength 40 Gbit/s supercontinuum was spectrum-sliced at λ_0(=1553.9 nm) using a 3 nm optical filter to convert into 40 Gbit/ TDM signal. To begin with the OTDM-to-WDM conversion, the measured optical spectrum and the corresponding temporal waveform of 40 Gbit/s OTDM are shown in Fig. 10(a) and 10(b), respectively. Figures 10(c) and 10(d) show the converted 4×10 Gbit/s WDM signals. Next, the WDM-to-TDM reconversion is performed in series and the experimental results are shown in Figs. 10(e) and 10(f). 40 Gbit/s TDM at λ_0 is converted to 10 Gbit/s WDM channels at λ_1–λ_4 and

reconverted to 40 Gbit/s OTDM at λ_0 with clear eye openings. All of the measured BERs of the converted four channel 10 Gbit/s WDM, and reconverted four channel 10 Gbit/s TDM data were less than 10^{-9}. Using the same technique with a supercontinuum generation, the OCDM-to-WDM and WDM-to-OCDM conversions were also demonstrated in [9].

5 Optical studies of photonic devices

Considering the broad bandwidth characteristics, supercontinuum light source is suitable for optical studies of photonic devices. As an example, we apply the supercontinuum light source to the study of nano-scale photonic crystal devices. Figure 11 shows the schematics of 1-D photonic crystal microcavity waveguide with an embedded point defect, whose optical characteristics were measured using a supercontinuum light source [10]. The supercontinuum light source used in the experiment is the same described in Section **2-3** [4]. Through the supercontinuum-based techniques, transmission measurements of the 1-D photonic crystal were obtainable over 800 nm bandwidths as shown in Fig. 12. An efficient, broadband waveguide coupling techniques and sensitive normalized detection enable rapid and high-resolution measurements of nano-scale one-dimensional photonic crystal microcavities. Experimental mappings of bandgaps and cavity mode resonances with a wavelength resolution of 0.1 nm compare well with computer simulations.

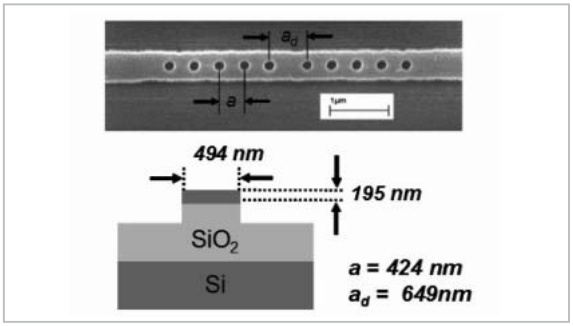

Fig.11 *1-D photonic crystal microcavity waveguide*

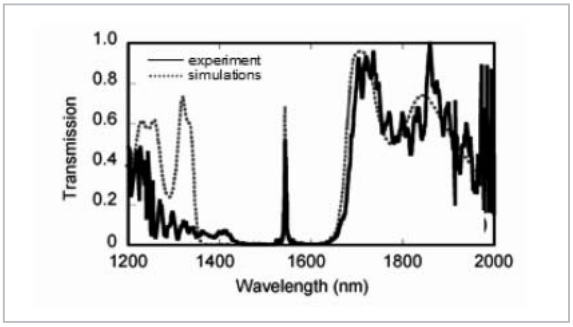

Fig.12 *Transmission characteristics of photonic crystal microcavity; measurement (solid) and simulation (dashed)*

6 Conclusion

In this paper the design theory of the supercontinuum generation in an optical fiber is described. Several applications of the supercontinuum for the photonic networks and optical sensing system were demonstrated. The demonstrated applications include multi-wavelength signal generation, tunable wavelength conversion, multiplexing format conversion, and optical studies of photonic devices. The demonstrations are based upon ultrafast photonic processing in time and frequency domain. A potential of ultra-high-speed operation, as well as the large scalability, distinguish the supercontinuum based schemes.

Acknowledgements

The author wishes to thank Prof. Ken-ichi Kitayama of Osaka University and Prof. Takeshi Ozeki of Sophia University for collaborations and useful discussions. The author also would like to thank Prof. Erich P. Ippen of Massachusetts Institute of Technology for his collaborations, valuable suggestions and encouragements.

References

1 S. Taccheo and L. Boivin, "Investigation and design rules of supercontinuum sources for WDM applications", Optical Fiber Communication Conference 2000, ThA1.

2 W. J. Tomlinson, R. H. Stolen, and C. V. Shank, "Compression of optical pulses chirped by self-phase modulation in fibers", J. Opt. Soc. Am. B. Vol 1, pp. 139-149, Apr. 1984.

3 J. T. Gopinath, H. M. Shen, H. Sotobayashi, E. P. Ippen, T. Hasegawa, T. Nagashima, and N. Sugimoto, "Highly nonlinear bismuth-oxide fiber for supercontinuum generation and femtosecond pulse compression", IEEE/OSA J. Lightwave Technol., Vol. 23, No. 11, pp. 3591-3596, 2005.

4 H. Sotobayashi, J. T. Gopinath, J. W. Sickler, and E. P. Ippen, "Broadband fiber lasers using Bismuth Oxide-based Erbium-doped fiber amplifiers", SPIE Optics East, paper 5595-03, Philadelphia, Oct. 2004.

5 H. Sotobayashi, A. Konishi, W. Chujo, and T. Ozeki, "Wavelength-band generation and transmission of 3.24-Tbit/s (81-channel WDM x 40-Gbit/s) carrier-suppressed return-to-zero format by use of a single supercontinuum source for frequency standardization", OSA J. Opt. Soc. Am. B, Vol. 19, No. 11, pp. 2803-2809, 2002.

6 H. Sotobayashi and K. Kitayama, "325 nm bandwidth supercontinuum generation at 10 Gbit/s using dispersion-flattened and non-decreasing normal dispersion fibre with pulse compression technique", IEE Electron. Lett., Vol. 34, No. 13, pp.1336-1337, 1998.

7 H. Sotobayashi, K. Kitayama, and W. Chujo, "Photonic gateway: TDM-to-WDM-to-TDM conversion and reconversion at 40 Gbit/s (4 channels 10 Gbits/s)", OSA J. Opt. Soc. Am. B, Vol. 19, No. 11, pp. 2810-2816, 2002.

8 H. Sotobayashi, W. Chujo, and T. Ozeki, "Wideband tunable wavelength conversion of 10 Gbit/s RZ signals by optical time-gating of highly chirped rectangular shape supercontinuum light source", OSA Opt. Lett., Vol. 26, No. 17, pp. 1314-1316, 2001.

9 H. Sotobayashi, W. Chujo, and K. Kitayama, "Photonic gateway: multiplexing format conversions of OCDM-to-WDM and WDM-to-OCDM at 40 Gbit/s (4 × 10 Gbit/s)", IEEE/OSA J. Lightwave Technol., Vol. 20, No. 12, pp. 2002-2008, 2002.

10 P. T. Rakich, H. Sotobayashi, J. T. Gopinath, S. G. Johnson, J. W. Sickler, C. W. Wong, J. D. Joannopoulos, and E. P. Ippen, "Nano-scale photonic crystal microcavity characterization with an all-fiber based 1.2-2.0 μm supercontinuum", OSA Optics Express, Vol. 13, No. 3, pp. 821-825, 2005.

***SOTOBAYASHI Hideyuki**, Dr. Eng.*

Senior Researcher, Advanced Communications Technology Group, New Generation Network Research Center (former : Senior Researcher, Photonic Information Technology Group, Basic and Advanced Research Department)

Ultrafast Photonic Processing, Photonic Network, Photonic Device